A NEW LOW-COMPLEXITY SUPER-RESOLUTION TECHNIQUE TO LOCALIZE TWO CLOSELY-SPACED PLANE-WAVE SOURCES

Mehrez Souden, Sofiène Affes, and Jacob Benesty

INRS-ÉMT, Université du Québec, Montréal, QC, Canada

ABSTRACT

We propose a new simple and accurate approach to localize two equipowered plane-wave sources (i.e., harmonics) using a uniform linear array (ULA) of sensors. We exploit the particular form of the covariance matrix jointly with a least square fitting (LSF) to derive new simple closed-form expressions for the directions of arrival (or harmonics in general). Simulation results demonstrate that resorting to this new method, mainly in the case of very low angular separation, and even with a limited number of sensors, leads to highly accurate results while requiring low computational complexity.

1. INTRODUCTION

Direction of arrival (DOA) estimation has attracted a lot of researchers' interest over the last few decades in several fields including radar detection, radiocommunications, satellite communications, etc. This fact is due to its inherent goal which consists in localizing spatially distributed sources by processing their mixtures at the receiving antenna array.

So far, numerous DOA estimation techniques have been developed. To illustrate, maximum-likelihood, covariance-matching, and asymptotically minimum variance-based algorithms have been proposed in [1, 2, 3], respectively. Despite their accuracy, these techniques generally require multidimensional non-linear optimizations leading to high computational complexity. Another well known trend has been to exploit the orthogonality between the noise and signal (plus noise) subspaces such as MUSIC [4] and its derivatives mainly root-MUSIC [5, 6] and a recently proposed root-MUSIC-like technique for non-circular sources [7, 8]. Compared to the former techniques, such approaches generally require low time and computational effort. Moreover, they do not require some restrictive assumptions on the observed signal such as their Gaussian or independence and identical distribution (i.i.d.) [2, 3]. Nevertheless, in the case of very closely-spaced sources, the performance of these methods deteriorates especially in adverse conditions [low signal-to-noise-ratio (SNR) and few sensors].

Figs. 2 and 3 illustrate this fact when the root-MUSIC and root-MUSIC-like (for non-circular sources) algorithms are used to localize two closely-spaced point sources. Notice, in addition, that the increase of the number of sensors enhances the accuracy of these techniques. Complete details of these results are provided in Section 5. This inevitable increased complexity may be prohibitive for the design of the receivers. Clearly, there is a need to develop a new method to deal with very low resolution problems without necessitating a large number of sensors neither high computational load or restrictive conditions (e.g., Gaussian or i.i.d. observations) to operate at very low SNR as in real-world practical applications.

In this paper, we present a new technique to localize two equipowered and closely-spaced point sources using a ULA of sensors. We use a LSF of the particular form of the observations' covariance matrix to establish new analytical expressions for the mean value of both spatial harmonics and their separation. Next, we deduce both DOAs in an optimal fashion. The resulting approach is simple and accurate even in adverse conditions (low SNR with few sensors deployed at the receiver).

We would like to emphasize that our special focus on this so called two-input multiple-output (TIMO) data model is motivated by the fact that it is practical in several situations where it is convenient to have less antennas at the transmitting end due to cost or space constraints or when antenna selection is performed [9]. Furthermore, the high accuracy of the proposed approach even with few sensors, as it will be shown in Section 5, accounts for its suitability to deal with several practical situations, among them: (i) *CDMA signature codes duplication*_ by implementing the proposed localization technique on the base station, the number of signature codes allocated to a single mobile terminal equipped with two closely-spaced multiplexing antenna elements could be doubled (combining both spatial signatures and the allocated signature codes) when scattering is negligible. (ii) *Angular spread estimation*_ for low angular spreads, it has been shown that estimating the angular spread and the nominal DOA of a single source amounts to the estimation of two closely-spaced DOAs with the same average power [10]. The current method is well suited for this application. (iii) *Satellites interference cancellation*_ thanks to its high accuracy, the proposed technique could be used to localize two interfering satellites with as low as 2^o angular separation (e.g., geostationary satellites) and, consequently, minimize their interference.

2. PROBLEM STATEMENT AND ASSUMPTIONS

We assume N stationary ergodic sources represented by an N-dimensional vector $\mathbf{s}(t) \triangleq [s_1(t) \ldots s_N(t)]^T$ and mixed by an $M \times N$ ($M > N$) channel matrix $\mathbf{A}$ to yield an M-dimensional vector of observations $\mathbf{x}(t) \triangleq [x_1(t) \ldots x_M(t)]^T$ at time t:

$$\mathbf{x}(t) \;=\; \mathbf{A}\,\mathbf{s}(t) + \mathbf{b}(t), \tag{1}$$

where $\mathbf{b}(t) \triangleq [b_1(t) \ldots b_M(t)]^T$ is an unknown noise vector composed of M Gaussian i.i.d centered stationary signals with variance σ_b^2. In the general DOA estimation scheme, the N sources are assumed to be narrow-band and impinging from different DOAs, $(\theta_l)_{1\le l\le N}$, on an antenna array composed of M sensors. In this work, we consider a ULA. Thus, the entries of the channel matrix, termed as steering matrix in this context, are expressed as:

$$a_{kn} = e^{j(k-1)\omega_n}; \forall\, 1 \le k \le M,\ 1 \le n \le N, \tag{2}$$

where $\omega_n \triangleq 2\pi\kappa\sin(\theta_n)$, and κ is the sensors separation in wavelengths ($\kappa = \frac{1}{2}$, generally). Source localization consists in recovering the N DOAs by solely processing the observations $\mathbf{x}(t)$. In the sequel, we will omit the time index t for the sake of clarity. We also stress that only the case of $N = 2$ is considered in this work[1]. Furthermore, we assume that the two sources are totally uncorrelated, and equi-powered (with $\sigma_s^2\mathbf{I}_2$ as a covariance matrix). This assumption holds in several practical situations, in particular, those mentioned in Section 1.

3. HARMONICS ESTIMATION USING THE PARTICULAR FORM OF THE COVARIANCE MATRIX

The theoretical covariance matrix of the resulting observations is given as:

$$\mathbf{R}_{\mathbf{x}} \triangleq \mathrm{E}\left\{\mathbf{x}\mathbf{x}^H\right\} = \sigma_s^2\mathbf{A}\mathbf{A}^H + \sigma_b^2\mathbf{I}_M. \tag{3}$$

Then,

$$\mathbf{R} \triangleq \mathbf{R}_{\mathbf{x}} - \sigma_b^2\mathbf{I}_M = \sigma_s^2\mathbf{A}\mathbf{A}^H. \tag{4}$$

In practice, $\mathbf{R}$ is unavailable, but can be estimated using a finite number, T, of samples as:

$$\hat{\mathbf{R}} = \frac{1}{T}\sum_{t=1}^{T}\mathbf{x}(t)\mathbf{x}^H(t) - \hat{\sigma}_b^2\mathbf{I}_M, \tag{5}$$

where $\hat{\sigma}_b^2$ is the estimate of σ_b^2 obtained by averaging over the $(M-2)$ smallest eigenvalues of the matrix $\hat{\mathbf{R}}_{\mathbf{x}} = \frac{1}{T}\sum_{t=1}^{T}\mathbf{x}(t)\mathbf{x}^H(t)$. Our new technique in localizing both equipowered sources is based on the explicit expression of the entries of $\mathbf{R}$ and the decomposition of ω_1 and ω_2 as:

$$\begin{cases} \omega_1 &= \omega - \delta_\omega \\ \omega_2 &= \omega + \delta_\omega \end{cases} \tag{6}$$

[1]We are currently investigating the general case $M \times N$.

where ω denotes the mean harmonic:

$$\omega = \frac{\omega_1 + \omega_2}{2}, \tag{7}$$

and $2\delta_\omega$ is the harmonics separation:

$$2\delta_\omega = |\omega_1 - \omega_2|. \tag{8}$$

Consequently, finding ω_1 and ω_2 amounts to finding ω and δ_ω. Here, we mainly focus on estimating ω and δ_ω. Using (7) and (8), the entry of the mth subdiagonal of $\mathbf{R}$, d_m, is expressed as:

$$d_m = 2\sigma_s^2\cos(m\delta_\omega)e^{jm\omega}. \tag{9}$$

To have better estimates of $(d_m)_{0\le m\le M-1}$, we exploit the Toeplitz structure of $\mathbf{R}$ by averaging over the $M-m$ entries of the mth subdiagonals of $\hat{\mathbf{R}}$. In other words, for $m \in \{0, \ldots, M-1\}$, d_m is estimated as:

$$\hat{d}_m = \frac{1}{M-m}\sum_{k=1}^{M-m}\hat{\mathbf{R}}(k+m, k). \tag{10}$$

To estimate δ_ω and ω, we use the following LSF of d_m, $1 \le m \le M-1$:

$$\hat{\omega}^{(m)},\ \hat{\delta}_\omega^{(m)} = \arg\min_{\omega,\ \delta_\omega} J_m(\omega, \delta_\omega) \tag{11}$$

where

$$J_m(\omega, \delta_\omega) \triangleq |\hat{d}_m - d_m|^2. \tag{12}$$

By setting the derivatives of $J_m(\omega, \delta_\omega)$ with respect to (w.r.t.) ω and δ_ω to zero and selecting the appropriate values (minimizing J_m), the above LSF leads to the following estimators:

$$\hat{\omega}^{(m)} = \frac{1}{m}\arg(\hat{d}_m) \pm \frac{2p\pi}{m}, \tag{13}$$

and

$$\hat{\delta}_\omega^{(m)} = \frac{1}{m}\arccos\left[\Re\left(\frac{\hat{d}_m}{\hat{d}_0}e^{-jm\omega}\right)\right]. \tag{14}$$

In (13), arg(.) and $\Re(.)$ stand for the angle and real part, respectively, $m \in \{1, \ldots, M-1\}$, $p \in \{0, \ldots, \lfloor\frac{m}{2}\rfloor\}$, and $\lfloor . \rfloor$ is the integer part operator. The superscript (m) is utilized for both estimators to specify that $\hat{d}_m$ is utilized in (13) and (14).

*Remark 1*_ The indetermination $\pm\frac{2p\pi}{m}$ in (13) does not appear for $\hat{\omega}^{(1)}$. If $\hat{d}_m$, $m > 1$, is utilized in (13), a set of $2\lfloor\frac{m}{2}\rfloor + 1$ possible values can be found for $\hat{\omega}^{(m)}$. To solve this indetermination, one has to use $\hat{\omega}^{(1)}$ as a reference value and chose the optimal estimator minimizing the distance $\left|\hat{\omega}^{(m)} - \hat{\omega}^{(1)}\right|$.

*Remark 2*_ The estimator (14) requires a prior knowledge of the range of δ_ω. Indeed, using (14), we suppose that:

$$\delta_\omega \le \frac{\pi}{2m}. \tag{15}$$

This condition is not restrictive as one can start by using the lowest values of m (first subdiagonals of $\hat{\mathbf{R}}$) to have a prior knowledge about the range of δ_ω then use the first obtained results as reference values before proceeding with the largest values of m. Finally, it is important to point out that the existing localization techniques are well performing for relatively high angular separations. This fact justifies our special focus on small angular (or equivalently harmonics) separations satisfying:

$$\delta_\omega < \frac{\pi}{2(M-1)}. \tag{16}$$

4. PERFORMANCE ANALYSIS

To gain some insights on the asymptotic performance of the proposed estimators, we assume as in [2] that the observations in (1) are circularly symmetric Gaussian i.i.d. This assumption leads to the following proposition.

Proposition 1 *Under the assumption of circularly symmetric Gaussian i.i.d. observations defined in (1), we have:*

$$\lim_{T\to+\infty} T\mathrm{E}\left\{\left(\hat{\omega}^{(m)}-\omega\right)^2\right\} = \frac{\tan^2(m\delta_\omega)}{2m^2} \tag{17}$$

$$\lim_{T\to+\infty} T\mathrm{E}\left\{\left(\hat{\delta}_\omega^{(m)}-\delta_\omega\right)^2\right\} = \frac{\frac{S(m,\delta_\omega)}{(M-m)^2}+\cos^2(m\delta_\omega)}{m^2\sin^2(m\delta_\omega)} \tag{18}$$

where

$$S(m,\delta_\omega) = \sum_{p,q=1}^{M-m}\cos\left[2(p-q)\delta_\omega\right]. \tag{19}$$

Cf. Appendix A for proof.

The variations of the asymptotical variances given in (17) and (18) are depicted in Fig. 1 for the case $M = 6$. Notice that the variance of $\hat{\omega}^{(m)}$ is increasing w.r.t. m and δ_ω when the condition (16) is satisfied. Hence, using the first subdiagonal of the covariance matrix leads to more accurate estimates of the central harmonic. In contrast, the asymptotical variance in (17) is decreasing w.r.t. m and δ_ω. Notice in addition that though the above asymptotical variances have been derived under the condition of circular Gaussian and i.i.d. observations, an extensive empirical investigation showed us that these monotonous variations are also observed when the above condition on the observations is not satisfied. From this, we derive our strategy in localizing both sources. Indeed, after calculating $\hat{\mathbf{R}}$, we use its first subdiagonal to calculate the central harmonic as in (7) (i.e., for $m = 1$) and the last subdiagonal to calculate the harmonics separation as in (14) (i.e., for $m = M-1$). Then, we estimate ω_1 and ω_2 as:

$$\left\{\begin{array}{lcl}\hat{\omega}_1 & = & \hat{\omega}^{(1)} - \hat{\delta}_\omega^{(M-1)} \\ \hat{\omega}_2 & = & \hat{\omega}^{(1)} + \hat{\delta}_\omega^{(M-1)}\end{array}\right. . \tag{20}$$

Both DOAs are deduced as $\hat{\theta}_n = \arcsin\left(\frac{\hat{\omega}_n}{2\kappa\pi}\right)$, $n \in \{1,\ 2\}$.

5. SIMULATION RESULTS

Along our simulations, we will use the root mean squared error (RMSE) as a performance index:

$$\mathrm{RMSE}(\theta_1,\theta_2) = \sqrt{\frac{1}{2\mathcal{M}}\sum_{\imath=1}^{\mathcal{M}}\sum_{n=1}^{2}\left|\theta_n - \hat{\theta}_n^{(\imath)}\right|^2}, \tag{21}$$

where $\left(\hat{\theta}_n^{(\imath)}\right)_{1\le n\le 2}$ are the estimates of $(\theta_n)_{1\le l\le 2}$ at the $\imath$th Monte-Carlo run ($1 \le \imath \le \mathcal{M}$), respectively. In all of the investigated scenarios, we take $\mathcal{M} = 5.10^2$. To have a better insight into the results, the RMSE and the CRLB values will be presented in degrees. We consider the scenario of two uncorrelated BPSK sources located at θ_1 and θ_2 as in [7, 8] (without loss of generality, $\theta_1 \le \theta_2$) with a ULA of 3 and 6 sensors. To estimate the required statistics as in (5), we use $T = 2.10^2$ samples of the observations of the two BPSK sources. We compare the proposed algorithm to root-MUSIC and one of its recently proposed variations (root-MUSIC-like) [7] for non-circular and uncorrelated sources (which is the case of the considered BPSK sources). The efficiency of the latter has been proved in [8] for this particular case. We also plot the square-root of the CRLB provided in [11] which is given in the investigated case of two equipowered BPSK sources with a ULA of sensors as:

$$\mathrm{CRLB}(\theta_n) \approx \sqrt{\frac{3\sigma_b^2}{2M(M^2-1)T\sigma_s^2\pi^2\kappa^2\cos^2(\theta_n)}}. \tag{22}$$

In Figs. 2 and 3, we plot RMSE(θ_1, θ_2) variations w.r.t. the angular separations, $\Delta\theta = \theta_2 - \theta_1$, (at SNR = 10 dB) and the SNR (at $\Delta\theta = 3°$), respectively, for 3 and 6 sensors. In both figures we notice that root-MUSIC's accuracy deteriorates when the signals are closely spaced or the SNR decreases. This fact is due to its inherent behavior that has been demonstrated in some earlier works [1, 6] where its variance is shown to take large values when the steering matrix is almost rank deficient (closely-spaced sources and/or low SNR). The root-MUSIC-like algorithm takes advantage of the non-circularity of the sources to provide more accurate results than the latter. However, its performance degrades in adverse conditions. In contrast, the proposed approach exhibits a regular behavior even with 3 sensors only and outperforms both algorithms. As one example, for an accuracy RMSE(θ_1, θ_2) $\approx 0.4°$, we clearly see in Fig. 3 that the latter requires SNR $\approx$ 14 and 3 dB when 3 and 6 sensors are deployed, while root-MUSIC requires SNR $\approx$ 30 and 14 dB, and the root-MUSIC-like requires SNR $\approx$ 25 and 8 dB, respectively. This fact illustrates the tremendous SNR gains achieved by the proposed method and the compactness it offers since it requires just 3 sensors to be as accurate as root-MUSIC operating with 6 sensors. Notice also that RMSE(θ_1, θ_2) achieved by the new method is lower bounded when the SNR is high. However, one should note that this is not actually a serious limitation since this lower bound is acceptable ($\approx 0.1°$) and appears only for very high SNR values rarely encountered in real-world practical applications (cf. Section 1).

6. CONCLUSION

In this paper, a new approach to localize two closely-spaced and equipowered plane-wave sources was presented. Based on a least square fitting of second order statistics of the observations, we established new closed form estimators for the mean value of the harmonics and their separation. Then, we deduced the angles of arrival of both sources in an optimal fashion (minimum asymptotical variance). The obtained results suggest that this new approach may be of great interest in several practical applications including satellites localization, CDMA signature codes duplication, angular spread estimation, etc.

7. REFERENCES

[1] P. Stoica and A. Nehorai, “MUSIC, maximum likelihood, and Cramer-Rao bound,” *IEEE Trans. Acoustics, Speech, Signal Process.*, vol. 37, no.5, pp. 720-741, May 1989.

[2] B. Ottersten, P. Stoica, and R. Roy, “Covariance matching estimation techniques for array signal processing applications,” *Digital Signal Process.*, vol. 8, no. 3, pp. 185-210, July 1998.

[3] J. P. Delmas, “Asymptotically minimum variance second-order estimation for non-circular signals with application to DOA estimation,” *Digital Signal Process.*, vol. 52, no. 5, pp. 1235-1241, May 2004.

[4] R. O. Schmidt, “Multiple emitter location and signal parameter estimation,” *IEEE Trans. Antennas & Propag.*, vol. 34, no. 3, pp. 276-280, Mar. 1986.

[5] A. J. Barabell, “Improving the resolution of eigenstructure-based direction finding algorithms,” in *Proc. IEEE ICASSP*, 1983, pp. 336-339.

[6] B. D. Rao and K. V. S. Hari, “Performance analysis of root-MUSIC,” *IEEE Trans. Acous., Speech, Signal Process.*, vol. 37, no. 7, pp. 1939-1949, Dec. 1989.

[7] P. Chargé, Y. Wang, and J. Saillard,“A non-circular sources direction finding method using polynomial rooting,” *Signal Process.,* vol. 81, no. 8, pp. 1765-1770, 2001.

[8] H. Abeida and J. P. Delmas, “MUSIC-like estimation of direction of arrival for non-circular sources,” *IEEE Trans. Signal Process.*, vol. 54, no. 7, pp. 2678-2690, July 2006.

[9] N. Wang and S. D. Blostein, “Minimum BER transmit optimization for two input multiple output spatial multiplexing,” in *Proc. IEEE Globecom*, 2005, vol. 6, pp. 3774-3778.

[10] M. Bengtsson and B. Ottersten, “Low-complexity estimators for distributed sources,” *IEEE Trans. Signal Process.*, vol. 48, no. 8, pp. 2185-2194, Aug. 2000.

[11] J. P. Delmas and H. Abeida, “Cramer-Rao bounds of DOA estimates for BPSK and QPSK modulated signals,” *IEEE Trans. Signal Process.,* vol. 54, no. 1, pp. 117-126, Jan. 2006.

[12] O. Besson, P. Stoica, and A. B. Gershman,“Simple and accurate direction of arrival estimator in the case of imperfect spatial coherence,” *IEEE Trans. Signal Process.,* vol. 49, no. 4, pp. 730-737, Apr. 2001.

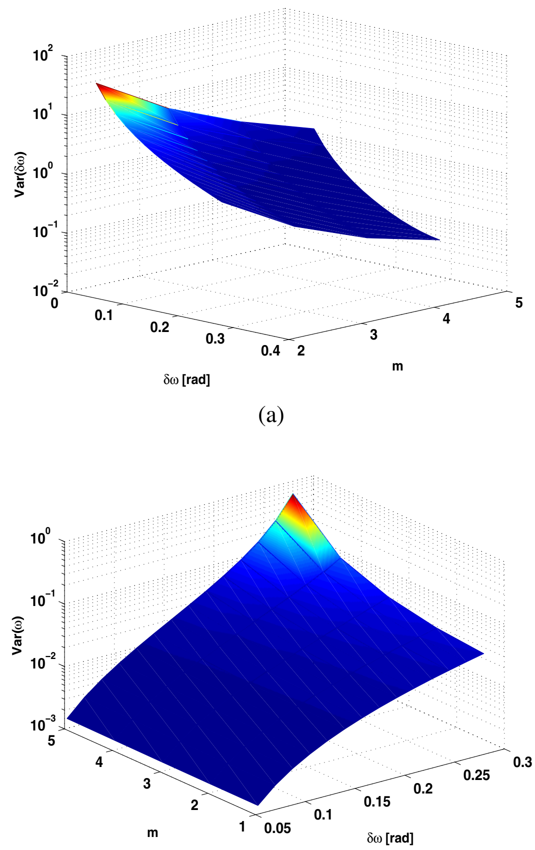

(a)

(b)

Fig. 1. Asymptotic variances of (a) $\hat{\delta}_\omega$ and (b) $\hat{\omega}$ w.r.t. δ_ω and m at $M = 6$ [cf. (23) and (24)].

A. APPENDIX: PROOF OF PROPOSITION 1

We derive the above results by proceeding as in [12] where the focus has been on the localization of a locally scattered source. Let $\xi_m = |d_m| = d_0 \cos(m\delta_\omega)$. Then, following [12], we can prove that:

$$\lim_{T\to+\infty} T\mathrm{E}\left\{\left(\hat{\omega}^{(m)} - \omega\right)^2\right\} = \frac{\lim_{T\to+\infty} T\mathrm{E}\left\{\left(\frac{\partial J_m}{\partial \omega}\right)^2\right\}}{\left[\lim_{T\to+\infty} \frac{\partial^2 J_m}{\partial \omega^2}\right]^2}, \quad (23)$$

and

$$\lim_{T\to+\infty} T\mathrm{E}\left\{\left(\hat{\delta}_\omega^{(m)} - \delta_\omega\right)^2\right\} = \frac{\lim_{T\to+\infty} T\mathrm{E}\{(\frac{\partial J_m}{\partial \delta_\omega})^2\}}{\left[\lim_{T\to+\infty} \frac{\partial^2 J_m}{\partial \delta_\omega^2}\right]^2}. \quad (24)$$

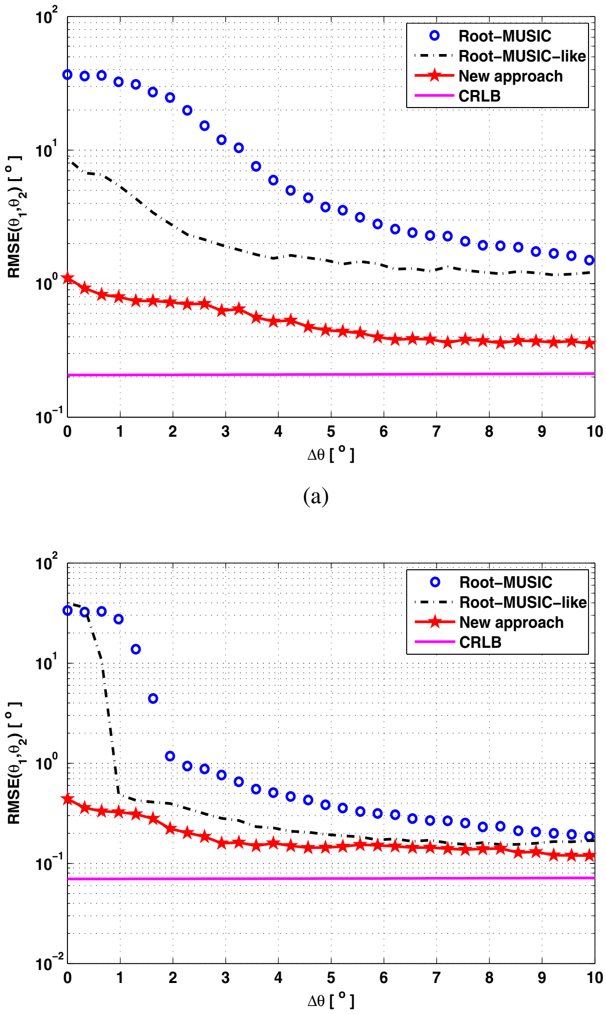

(a)

(b)

Fig. 2. Performance of the proposed method compared to root-MUSIC and root-MUSIC-like algorithms w.r.t. $\Delta\theta$, at SNR $=$ 10 dB using: (a) 3 sensors, and (b) 6 sensors.

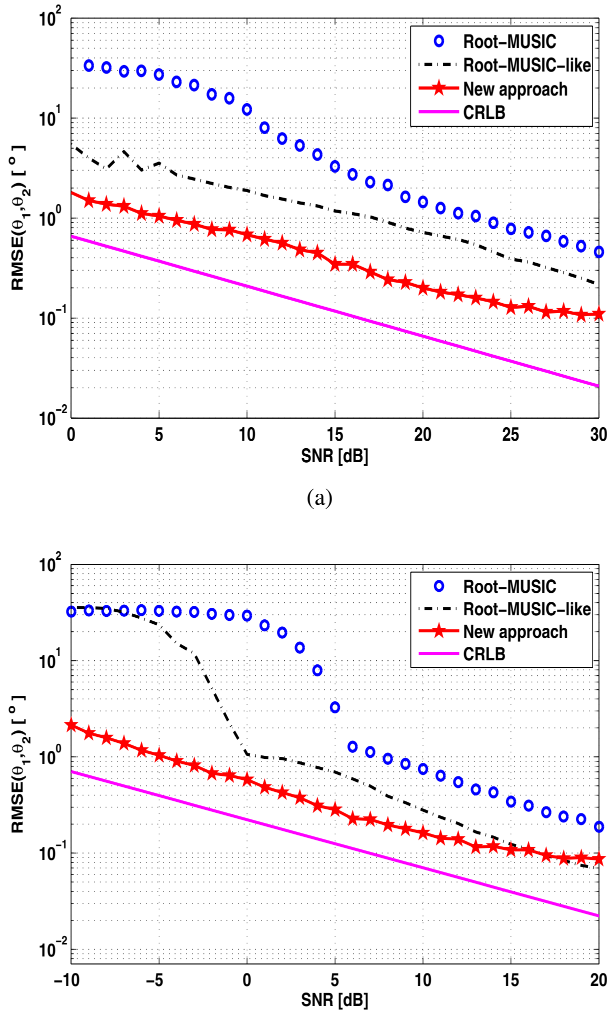

(a)

(b)

Fig. 3. Performance of the proposed method compared to root-MUSIC and root-MUSIC-like algorithms w.r.t. SNR, at $\Delta\theta = 3^\circ$ using: (a) 3 sensors, and (b) 6 sensors.

The above derivatives are evaluated at the actual parameters. Next, it can be shown using (12) that $\frac{\partial J_m}{\partial \omega} = -2m\xi_m \Im\{\hat{d}_m e^{-jm\omega}\}$, $\frac{\partial^2 J_m}{\partial \omega^2} = 2m^2\xi_m \Re\{\hat{d}_m e^{-jm\omega}\}$, $\frac{\partial J_m}{\partial \delta_\omega} = -2md_0\sin(m\delta_\omega)\left[\xi_m - \Re(\hat{d}_m e^{-jm\omega})\right]$, and $\frac{\partial^2 J_m}{\partial \delta_\omega^2} = 2m^2 d_0^2 \sin^2(m\delta_\omega) - 2m^2\xi_m\left[\xi_m - \Re(\hat{d}_m e^{-jm\omega})\right]$. Using the i.i.d. property of the observations it can be shown that $\lim\limits_{T\to+\infty} \frac{\partial^2 J_m}{\partial \omega^2} = 2m^2\xi_m^2$, and $\lim\limits_{T\to+\infty} \frac{\partial^2 J_m}{\partial \delta_\omega^2} = 2m^2 d_0^2 \sin^2(m\delta_\omega)$. To calculate the numerators in (23) and (24), we use the circular Gaussian and i.i.d. property of the observations jointly with the fact that for a given complex variable χ, $\Re^2(\chi) = \frac{1}{2}\left[|\chi|^2 + \Re(\chi^2)\right]$ and $\Im^2(\chi) = \frac{1}{2}\left[|\chi|^2 - \Re(\chi^2)\right]$. Here, $\Im(.)$ denotes the imaginary part. After some tedious calculations, we find that $\lim\limits_{T\to+\infty} TE\left\{(\frac{\partial J_m}{\partial \omega})^2\right\} = 2m^2 d_0^2 \xi_m^2 \sin^2(m\delta_\omega)$ and $\lim\limits_{T\to+\infty} TE\{(\frac{\partial J_m}{\partial \delta_\omega})^2\} = 4m^2 d_0^4 \sin^2(m\delta_\omega)\left[\cos^2(m\delta_\omega) + \frac{S(m,\delta_\omega)}{(M-m)^2}\right]$, where $S(m,\delta_\omega)$ is as defined in (19). Injecting these limits in (23) and (24), we obtain (17) and (18).